Inorg. Chem. **2006**, *45*, 1367–1379

Reactivity of Aquacobalamin and Reduced Cobalamin toward *S*-Nitrosoglutathione and *S*-Nitroso-*N*-acetylpenicillamine

Maria Wolak,[†,‡] Grażyna Stochel,*[,†] and Rudi van Eldik*[,‡]

Faculty of Chemistry, Jagiellonian University, 30060 Krakow, Poland, and Institute for Inorganic Chemistry, University of Erlangen-Nürnberg, Egerlandstrasse 1, 91058 Erlangen, Germany

Received August 1, 2005

The reactions of aquacobalamin (Cbl(III)H_2O, vitamin B_{12a}) and reduced cobalamin (Cbl(II), vitamin B_{12r}) with the nitrosothiols *S*-nitrosoglutathione (GSNO) and *S*-nitroso-*N*-acetylpenicillamine (SNAP) were studied in aqueous solution at pH 7.4. UV–vis and NMR spectroscopic studies and semiquantitative kinetic investigations indicated complex reactivity patterns for the studied reactions. The detailed reaction routes depend on the oxidation state of the cobalt center in cobalamin, as well as on the structure of the nitrosothiol. Reactions of aquacobalamin with GSNO and SNAP involve initial formation of Cbl(III)–RSNO adducts followed by nitrosothiol decomposition via heterolytic S–NO bond cleavage. Formation of Cbl(III)(NO^-) as the main cobalamin product indicates that the latter step leads to efficient transfer of the NO^- group to the Co(III) center with concomitant oxidation of the nitrosothiol. Considerably faster reactions with Cbl(II) proceed through initial Cbl(II)–RSNO intermediates, which undergo subsequent electron-transfer processes leading to oxidation of the cobalt center and reduction of the nitrosothiol. In the case of GSNO, the overall reaction is fast ($k \approx 1.2 \times 10^6$ M^{-1} s^{-1}) and leads to formation of glutathionylcobalamin (Cbl(III)SG) and nitrosylcobalamin (Cbl(III)(NO^-)) as the final cobalamin products. A mechanism involving the reversible equilibrium Cbl(II) + RSNO $\rightleftarrows$ Cbl(III)SR + NO is suggested for the reaction on the basis of the obtained kinetic and mechanistic information. The corresponding reaction with SNAP is considerably slower and occurs in two distinct reaction steps, which result in the formation of Cbl(III)(NO^-) as the ultimate cobalamin product. The significantly different kinetic and mechanistic features observed for the reaction of GSNO and SNAP illustrate the important influence of the nitrosothiol structure on its reactivity toward metal centers of biomolecules. The potential biological implications of the results are briefly discussed.

Introduction

S-Nitrosothiols belong to the group of organic nitroso compounds with the general structure R−X−N═O (X = C, S, N, and O donors). Although the first syntheses of nitrosothiols were carried out more than a century ago, interest in these compounds has been stimulated by discoveries of the in vivo synthesis and physiological functions of NO. Studies in this field revealed numerous connections between the biochemistry of nitrosothiols and that of NO.[1−6] In particular, thiols and nitrosothiols have been shown to participate in the storage, transport, and redox modifications of NO in vivo and thus are relevant to the physiological processes involved in blood pressure control, neurotransmission, and immune defense.[1−4] Since nitrosothiols may undergo a number of reactions under physiological conditions which lead to the release of nitric oxide or its redox-related forms, NO^+ and NO^-, they also have a potential medical application as NO donors.[1−6] The processes leading to donation of NO from a nitrosothiol may involve both homolytic and heterolytic cleavage of the S−NO bond, as outlined in Scheme 1.

Scheme 1

$$RS\text{-}NO \rightarrow RS^{\bullet} + NO^{\bullet} \quad \text{homolytic bond cleavage}$$

$$\left.\begin{array}{l} RS\text{-}NO \rightarrow RS^{+} + NO^{-} \\ RS\text{-}NO \rightarrow RS^{-} + NO^{+} \end{array}\right\} \quad \text{heterolytic bond cleavage}$$

* To whom correspondence should be addressed.
† Jagiellonian University.
‡ University of Erlangen-Nürnberg.

(1) Wang, G. P.; Xian, M.; Tang, X.; Wu, X.; Wen, Z.; Cai, T.; Janczuk, A. J. *Chem. Rev.* **2002**, *102*, 1091 and references therein.
(2) Williams, D. L. H. *Acc. Chem. Res.* **1999**, *32*, 869 and references therein.
(3) Hogg, N. *Free Radical Biol. Med.* **2000**, *28*, 1478 and references therein.
(4) Butler, A. R.; Rhodes, P. *Anal. Biochem.* **1997**, *249*, 1 and references therein.
(5) Richter-Addo, G. B. *Acc. Chem. Res.* **1999**, *32*, 529 and references therein.
(6) Szaciłowski, K.; Stasicka, Z. *Prog. React. Kinet. Mech.* **2000**, *26*, 1 and references therein.

10.1021/ic051300q CCC: $33.50 © 2006 American Chemical Society
Published on Web 12/23/2005

Importantly, these processes can be promoted by transition metal complexes and may occur according to a variety of mechanisms, owing to various modes in which RSNO may coordinate to the metal center (the actual coordination mode depending on the nature of the metal and the nitrosothiol structure).[1,2,5−7] Both S- and N-bonded metal−RSNO adducts may undergo subsequent homolytic or heterolytic cleavage of the S−NO bond, and these reactions can be accompanied by a change in the oxidation state of the metal center. Due to the possible biological relevance of such interactions, considerable attention has been given to metal-ion-catalyzed decomposition of nitrosothiols.[6−13] Although the physiological activity of nitrosothiols is usually attributed to the release of free NO, recent experimental results suggest that RSNO's may transfer the NO group through direct binding to the biologically relevant metal centers without generation of free NO.[12] Such a direct transfer of NO to the metal center has recently been established in the reactions of nitrosothiols with selected non-heme iron complexes and Ru, Os, and Fe heme models.[5−13]

The nature of intermediates and ultimate reaction products of metal−RSNO interactions was observed to depend both on the electronic configuration and redox properties of the metal center and on the structure of the nitrosothiol. Experimental data available to date are, however, not sufficient to allow a good correlation of these factors with the observed reaction mechanisms.

In this paper, we report and discuss the results of semiquantitative kinetic studies on the reactions of aquacobalamin, Cbl(III)H_2O, and its one-electron reduced form, Cbl(II) with *S*-nitrosoglutathione (GSNO) and *S*-nitroso-*N*-acetylpenicillamine (SNAP) (Figure 1) performed in aqueous solutions at the physiological pH 7.4. The nitrosothiols selected for the study belong to the most commonly used sources of NO in the biomedical field. Both GSNO and SNAP exhibit strong hypotensive effects, as well as other physiological actions which mimic those of NO.[1−4,14] Studies on the interactions of GSNO with cobalamins presented here were performed (i) to elucidate the nature of the chemical processes leading to the reported stimulation of the NO-donating activity of GSNO in the presence of cobalamin[15,16]

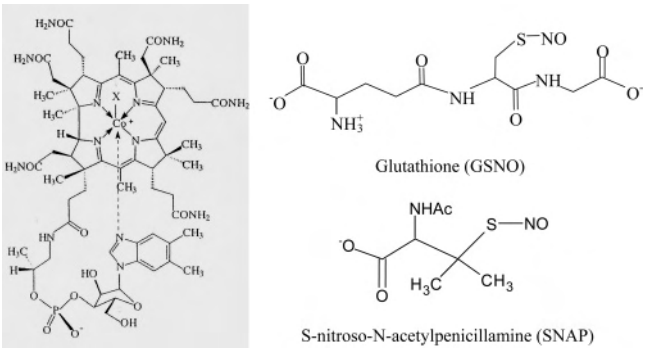

Figure 1. Structure of cobalamin (Co^{3+}, X = H_2O—aquacobalamin, Cbl(III)H_2O; Co^{2+}—reduced cobalamin, Cbl(II), a five-coordinate complex) and studied nitrosothiols (ionization of the carboxylic and amine groups indicated in the figure refers to physiological pH). The overall charges of Cbl(III)H_2O (+1) and nitrosothiols (−1) were omitted for clarity in equations and schemes throughout the text.

and (ii) to gain insight into the mechanism of NO interaction with glutathionylcobalamin, a naturally occurring vitamin B_{12} form present in mammalian cells,[17−20] which has been shown to react with NO.[21] The latter reaction, suggested to occur according to eq 1, was proposed as a likely pathway for cobalamin-mediated inhibition of the physiological activity of NO.[21]

$$\text{Cbl(III)SG} + \text{NO} \rightarrow \text{Cbl(III)}(\text{NO}^-) + {}^{\bullet}\text{SG} \qquad (1)$$

A more general goal of the study was to provide information on the reactivity of GSNO toward the low-spin Co(III) and Co(II) centers in aquacobalamin (vitamin B_{12a}) and reduced cobalamin (vitamin B_{12r}), respectively, that would allow comparison with other metal−RSNO systems.

To assess the effect of the nitrosothiol structure on its reactivity toward the Co(III) and Co(II) center, reactions of Cbl(III)H_2O and Cbl(II) with *N*-acetylated tertiary nitrosothiol SNAP (whose structural and electronic features are significantly different from that of GSNO)[6,22,23] were also studied, and the results are compared with those obtained for GSNO.

Experimental Section

Materials. Hydroxocobalamin hydrochloride (≥98%), GSNO[24] (≥97%), SNAP[24] (≥97%), reduced glutathione (≥99%), and

(7) Lee, J.; Chen, L.; West, A. H.; Richter-Addo, G. B. *Chem. Rev.* **2002**, *102*, 1019 and references therein.
(8) Butler, A. R.; Elkins-Daukes, S.; Parkin, D.; Williams, D. L. H. *Chem. Commun.* **2001**, 1732.
(9) Vilhena, F. S.; Louro, S. R. W. *J. Inorg. Biochem.* **2004**, *98*, 459.
(10) (a) Yi, G.-B.; Chen, L.; Khan, M. A.; Richter-Addo, G. B. *Inorg. Chem.* **1997**, *36*, 3876. (b) Chen, L.; Khan, M. A.; Richter-Addo, G. B. *Inorg. Chem.* **1998**, *37*, 533.
(11) (a) Yi, G.-B.; Khan, M. A.; Powell, D. R.; Richter-Addo, G. B. *Inorg. Chem.* **1998**, *37*, 208. (b) Lee, J.; Yi, G.-B.; Khan, M. A.; Richter-Addo, G. B. *Inorg. Chem.* **1999**, *38*, 4578.
(12) Cheng, L.; Richter-Addo, G. B. Binding and activation of nitric oxide by metalloporphyrins and heme. In *The Porphyrin Handbook*; Kadish, K. M., Smith, K. M., Guilard, R., Eds.; Academic Press: New York, 1999; Vol. 4 and references therein.
(13) Andreasen, L. V.; Lorkovic, I. M.; Richter-Addo, G. B.; Ford, P. C. *Nitric Oxide, Biol. Chem.* **2002**, *6*, 228.
(14) Smith, J. N.; Dasgupta, T. P. *Nitric Oxide, Biol. Chem.* **2000**, *4*, 57 and references therein.
(15) (a) Jenkinson, K. M.; Reid, J. J.; Rand, M. J. *Eur. J. Pharmacol.* **1995**, *275*, 145. (b) Li, C. G.; Rand, M. J. *Clin. Exp. Pharmacol. Physiol.* **1993**, *20*, 633. (c) Rand, M. J.; Li, C. G. *Eur. J. Pharmacol.* **1993**, *241*, 249.
(16) De Man, J. G.; Boeckstaens, G. E.; De Winter, B. Y.; Moreels, T. G.; Misset, M. E.; Herman, A. G.; Pelckmans, P. A. *Br. J. Exp. Therap.* **1995**, *114*, 1179.
(17) Xia, L.; Cregan, A. G.; Berben, L. A.; Brasch, N. E. *Inorg. Chem.* **2004**, *43*, 6848.
(18) Pezacka, E.; Green, R.; Jacobsen, D. W. *Biochem. Biophys. Res. Commun.* **1990**, *169*, 443.
(19) (a) Pezacka, E. H.; Jacobsen, D. W.; Luce, K.; Green, R.; *Biochem. Biophys. Res. Commun.* **1992**, *184*, 832. (b) Pezacka, E. H. *Biochim. Biophys. Acta* **1993**, *1157*, 167.
(20) Jacobsen, D. W.; Lee-Denison, C.; Luce, K.; Green, R. *Fed. Proc.* **1987**, *46*, 1005.
(21) Zheng, D.; Birke, R. L. *J. Am. Chem. Soc.* **2002**, *124*, 9066.
(22) Konorev, E. A.; Kalyanaraman, B.; Hogg, N. *Free Radical Biol. Med.* **2000**, *28*, 1671.
(23) Wang, K.; Hou, Y.; Zhang, W.; Ksebati, M. B.; Xian, M.; Cheng, J.-P.; Wang, P. G. *Bioorg. Med. Chem. Lett.* **1999**, *9*, 2897.

N-acetylpenicillamine (NAP, ≥99%) were obtained from Sigma and were used without further purification. Sodium formate, Na_2(edta), and other chemicals used throughout this study were of analytical reagent grade.

Solutions of nitrosothiols were prepared freshly before measurements by dissolving a weighted amount of nitrosothiol in Tris-$HClO_4$ (0.1 M) or phosphate buffer (0.1 M) containing Na_2(edta) (1×10^{-4} M) and were protected from exposure to ambient light before and during measurements. Solutions of Cbl(II) were prepared by chemical reduction of aquacobalamin with sodium formate under inert atmosphere and subsequent dilution of the stock solution with deoxygenated buffer to the appropriate concentration. Due to the marked oxygen sensitivity of NO, Cbl(II), and Cbl(III)(NO^-) (nitrosylcobalamin occurring as one of the products), solutions were prepared and handled in the absence of O_2 (with the use of Schlenk techniques) unless otherwise stated. Oxygen-free argon and nitrogen were used to remove oxygen. All solutions were prepared from deionized (Millipore) or triply distilled water.

Measurements. All kinetic experiments were performed under pseudo-first-order conditions, i.e., at least a 10-fold excess of nitrosothiol. Stopped-flow measurements were performed by rapidly mixing solutions of the reactants using an SX-17MV (Applied Photophysics) spectrophotometer thermostated to ±0.1 °C. The observed rate constants were mean values of at least five kinetic runs. Low-temperature time-resolved spectra were recorded with a Hi-Tech SF-3L low-temperature stopped-flow unit (Hi-Tech Scientific, Salisbury, U.K.) equipped with a J&M TIDAS 16/300-1100 diode array spectrophotometer (J&M, Aalen, Germany). High-pressure stopped-flow experiments were performed at pressures up to 130 MPa on a custom-built stopped-flow unit[25] thermostated to ±0.1 °C. Kinetic traces were recorded on an IBM-compatible computer and analyzed with the OLIS KINFIT (Bogart, GA) set of programs.

UV−vis spectral changes and slow reaction kinetics were monitored in gastight cuvettes in the thermostated (±0.1 °C) cell compartment of a Shimadzu UV-2001 spectrophotometer. ^{1}H and ^{31}P NMR spectra were recorded on a Bruker Avance DPX300 NB spectrometer operating at 300.13 and 121.5 MHz for ^{1}H and ^{31}P NMR, respectively. Chemical shifts were referenced internally to TSP (trimethylsilyl propionate, ^{1}H NMR) and TMP (trimethyl phosphate, ^{31}P NMR). The apparent pH was adjusted by addition of NaOD.

Cyclic voltammograms were recorded using an EG&G Princeton Applied Research Model 263 potentiostat. All measurements were performed at room temperature under nitrogen atmosphere in a VC-2 voltammetry cell (Bioanalytical Systems) with a standard three-electrode configuration. Pt wire and a glassy carbon disk electrode (3.0 mm diameter) were used as counter and working electrodes, respectively. The potentials are referenced to an aqueous Ag/AgCl electrode ($E° = 0.222$ V). Phosphate buffer (0.1 M) was used as supporting electrolyte.

The release of NO resulting from addition of a nitrosothiol to a solution of Cbl(III)H_2O and Cbl(II) was monitored with the isolated nitric oxide meter (WPI Instruments, model ISO-NO) calibrated according to the procedure described in the suppliers manual (generation of NO from $NaNO_2$ in the presence of an excess of KI at acidic pH). Measurements were performed in the dark under oxygen-free conditions.

The stability constant of the Cbl(III)SR adduct of cobalamin with NAP was determined at 25 °C in air-equilibrated 0.1 M phosphate buffer (pH 7.0) by spectrophotometric titration of aquacobalamin (9×10^{-5} M) with NAP ($0-9 \times 10^{-3}$ M, 0−100 mol equiv).

Results and Discussion

Reaction of Cbl(III)H_2O with *S*-Nitrosoglutathione. The reaction of aquacobalamin with GSNO was studied at pH 7.4 by UV−vis and NMR spectroscopy. Initial UV−vis measurements performed in the absence of O_2 evidenced the occurrence of at least two distinct reaction steps. In addition, the pattern of UV−vis spectral changes depended strongly on the oxygen content of the sample. Figure 2a reports typical spectral changes accompanying the reaction of aquacobalamin and GSNO in the absence of O_2. The first reaction step observed under such conditions was evidenced by small shifts in the spectrum of Cbl(III)H_2O (absorbance increase in the region 450−530 and 530−650 nm with concomitant decrease in absorbance at ca. 350 and 450−520 nm, inset in Figure 2a) which occurred on a time scale of several minutes. The second, slower step clearly involved formation of significant amounts of nitrosylcobalamin, Cbl(III)(NO^-)[26] as evidenced by absorbance increase at 258, 288, and 320 nm and in the spectral range 420−480 nm.[26b] The final UV−vis spectrum evidenced the presence of Cbl(III)SG and Cbl(III)(NO^-) as the reaction products, from which the latter could be easily oxidized to Cbl(III)NO_2 by allowing air into the solution. The resulting spectrum resembled that recorded for a mixture of glutathionylcobalamin, Cbl(III)SG,[27] and nitrocobalamin, Cbl(III)NO_2, prepared in a separate experiment by equilibration of glutathionylcobalamin with excess NO_2^- (eq 2).

$$\text{Cbl(III)SG} + NO_2^- + H^+ \rightleftarrows \text{Cbl(III)}NO_2 + \text{GSH} \quad (2)$$

Figure 2b shows a representative example of the UV−vis spectral changes resulting from mixing of air-saturated

(24) Possible interference of NO_2^-/RSH/RSSR impurities that could be present at the 1−3% level in the RSNO reactants has been considered. Results of elemental analysis of GSNO (C 36.2%, calcd 35.7%; N 16.7%, calcd 16.6%) and SNAP (C 38.5%, calcd 38.1%; N 12.0%, calcd 12.7%) indicate that the nitrosothiols used in our studies are not contaminated with nitrite and possibly contain only residual amounts of impurities such as RSH or RSSR. Any significant contribution of NO_2^-/RSH/RSSR contaminants to the observed reactivity patterns can be excluded on the basis of the NMR experiments in which equimolar (or nearly equimolar) concentrations of RSNO and cobalamin were reacted. The quantitative conversion of Cbl(III)H_2O and Cbl(II) to the final cobalamin products observed in these experiments (as described in the Results and Discussion section) cannot be induced by 1−3% of NO_2^-/RSH/RSSR contaminants introduced with the nitrosothiol reactant but apparently reflects the intrinsic reactivity of cobalamin towards RSNO. Additional blank UV−vis experiments in which Cbl(III)H_2O and Cbl(II) (ca. 5×10^{-5} M) were reacted with low concentrations of the potential contaminants (2×10^{-5} M RSH + 2×10^{-5} M NO_2^-, pH 7.4) in the absence of RSNO confirmed that the UV−vis kinetic and spectroscopic data reported in our work reflect the reactivity of RSNO toward Cbl(III)H_2O and Cbl(II) and are not artifacts introduced by contaminations of the nitrosothiol reactants.

(25) Spitzer, M.; Gartig, F.; van Eldik, R.; *Rev. Sci. Instrum.* **1988**, *59*, 2092.

(26) (a) The same product (representing a {CoNO}^{8} nitrosyl according to Enemark and Feltham notation) can be also formed by reacting Cbl(II) with NO and thus can be denoted as Cbl(II)NO. However, since its electronic properties are better described by the formula Cbl(III)(NO^-) according to which the nitroxyl ligand NO^- is coordinated to the formally Co(III) center (compare ref 26b), the latter notation is used in the text. (b) Wolak, M.; Zahl, A.; Schneppensieper, T.; Stochel, G.; van Eldik, R. *J. Am. Chem. Soc.* **2001**, *123*, 9780.

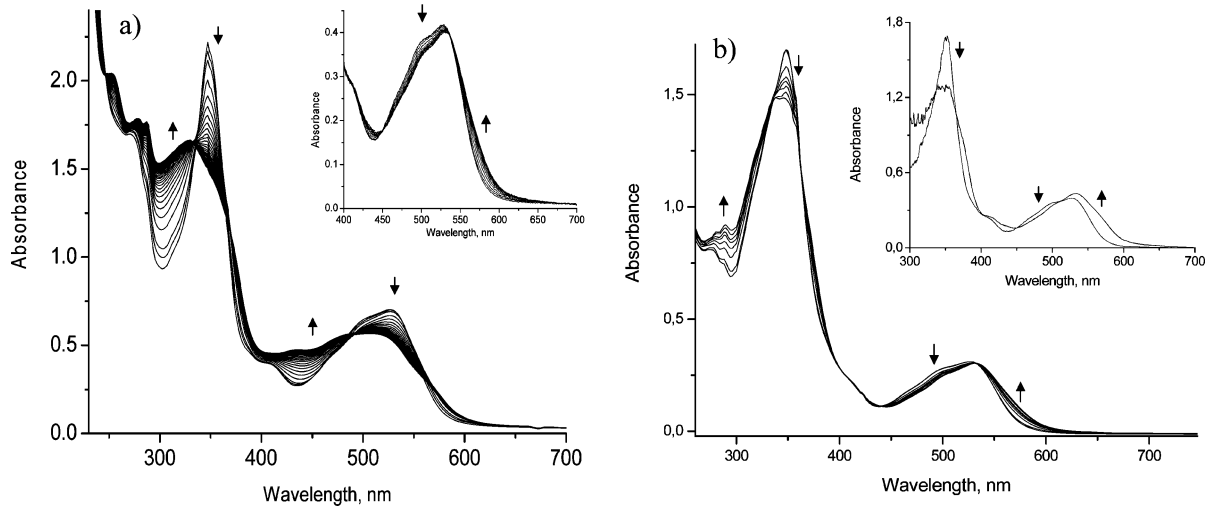

Figure 2. (a) UV−vis spectral changes accompanying the reaction of Cbl(III)H_2O (1×10^{-4} M) with GSNO (1×10^{-3} M) in deoxygenated solution at pH 7.4. The inset shows the spectral changes in the region 400−700 nm featuring the first reaction step. (b) The UV−vis spectral evolution observed in the first step of the reaction of Cbl(III)H_2O (5×10^{-5} M) with GSNO (1×10^{-3} M) in the presence of O_2. The inset shows the overall spectral change observed within 60 h after mixing of the reactants.

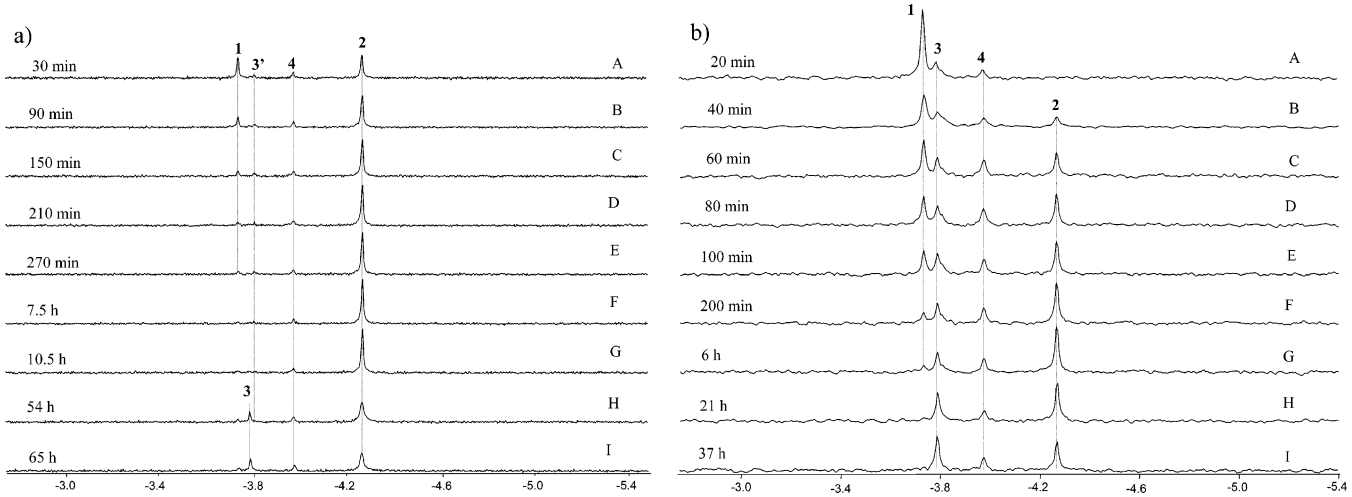

Figure 3. Time evolution of the ^{31}P NMR spectra during the reaction of GSNO (1 mM) with Cbl(III)H_2O (1 mM) at pH 7.4 (0.1 M Tris) in the absence (a) and presence of O_2 (b). Peak assignments (based on ^{31}P and ^{1}H NMR spectra of authentic cobalamins, compare Table S1): **1**, Cbl(III)H_2O; **2**, Cbl(III)(NO^-); **3**, Cbl(III)NO_2; **3′**, Cbl(III)NO_2 or Cbl(III)-N(O)SG; **4**, Cbl(III)SG. The time elapsed after mixing of the reactants is specified on the left side of the figures; $T = 25$ °C.

solutions of Cbl(III)H_2O and GSNO. The pattern of spectral changes featuring the first reaction step under such conditions resembled that observed in the absence of oxygen. The subsequent processes occurring on a time scale of several hours led to the final UV−vis spectrum which was different from that formed in the absence of oxygen (inset in Figure 2b). The lack of isosbestic points in the spectral changes featuring the slow phase of the reaction indicates the occurrence of at least two reaction paths during which the concentration of the absorbing species changes.

The nature of intermediates and products occurring in the reaction was further investigated by NMR spectroscopy. This involved analysis of diagnostic aromatic ^{1}H shifts of cobalamin species[28,29] formed at different stages of the reaction and their corresponding ^{31}P spectra (two typical examples of NMR spectra observed for the studied system and reference data on the aromatic ^{1}H shifts and ^{31}P resonances of selected cobalamin complexes which were used for peak assignments[27a,28] are reported in Figure S1 and Table S1 in the Supporting Information). Due to simplicity of the ^{31}P NMR spectra of various Cbl(III)X derivatives, which exhibit a single ^{31}P signal originating from the phosphodiester moiety of cobalamin[28b,29] (compare Figure 1) at positions depending on the nature of the axial ligand X, the cobalamin species formed in the reaction will be discussed on the basis of ^{31}P NMR data (for which, however, the ^{31}P peak assignments were verified by ^{1}H NMR spectroscopy). Figure 3 shows the evolution of ^{31}P NMR spectra observed after mixing of deoxygenated (Figure 3a) and air-saturated (Figure 3b)

(27) For the characteristic UV−vis spectrum of glutathionylcobalamin, compare (a) Brasch, N. E.; Hsu, T.-L. C.; Doll, K. M.; Finke, R. G. *J. Inorg. Biochem.* **1999**, *76*, 197. (b) Adler, N.; Medwick, T.; Poznanski, T. J. *J. Am. Chem. Soc.* **1966**, *88*, 5018.

(28) (a) Brasch, N. E.; Finke, R. G. *J. Inorg. Biochem.* **1999**, *73*, 215 and references therein. (b) Rossi, M.; Glusker, J. P.; Randaccio, L.; Summers, M. F.; Toscano, P. J.; Marzilli, L. G. *J. Am. Chem. Soc.* **1985**, *107*, 1729 and references therein.

(29) Brown, K. L. NMR Spectroscopy of B_{12}. In *Chemistry and Biochemistry of B_{12}*; Banerjee, R., Ed.; John Wiley and Sons: New York, 1999.

Scheme 2

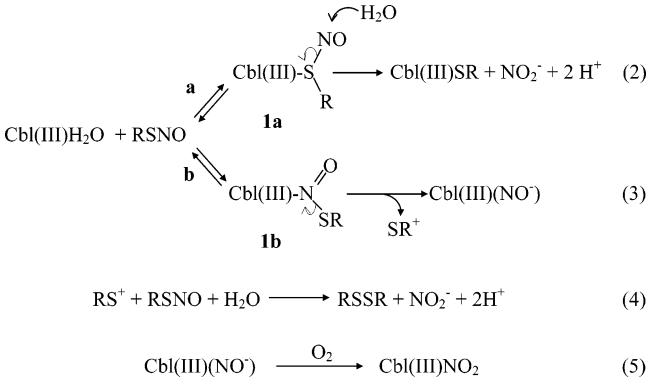

solutions of aquacobalamin and GSNO. Trace A in Figure 3a shows the spectrum of Cbl(III)H_2O 30 min after addition of GSNO. At this stage, aquacobalamin (^{31}P peak at −3.66 ppm) has partially reacted, and three new species with ^{31}P resonances at −4.25, −3.96, and −3.80 ppm can be detected. The species with an intense resonance at −4.25 ppm is easily identified as Cbl(III)(NO^-) (compare Table S1). The ^{31}P signals of the remaining two species appear at positions nearly identical with those of glutathionylcobalamin (−3.95 ppm) and nitrocobalamin (Cbl(III)NO_2, −3.77 ppm) prepared independently under the same experimental conditions. The very low-intensity peak at −3.80 ppm is ascribed to small amounts of Cbl(III)NO_2 formed in the initial stages of the reaction or to the transient N-bound intermediate Cbl(III)N(O)SR assumed to be present at low concentrations in the reaction mixtures (compare Scheme 2, eq 3). On a longer time scale, aquacobalamin is converted to Cbl(III)(NO^-), which is the predominant reaction product. This is accompanied by only minor changes in the intensity of the peak at −3.96 ppm, while the small signal at −3.80 ppm disappears at the final stage of the reaction. On a significantly longer time scale (6−70 h), the decrease in the intensity of the signal at −4.25 ppm, accompanied by appearance of a peak at −3.77 ppm indicates an onset of a slow oxidation of Cbl(III)(NO^-) to Cbl(III)NO_2 (traces H−I in Figure 3a). This results from slow diffusion of O_2 into the NMR tube or represents the internal reactivity of the system (e.g., oxidation of Cbl(III)(NO^-) by RSSR formed as a product of nitrosothiol decomposition). The analogous spectra recorded for air-equilibrated solutions (Figure 3b) indicate that Cbl(III)(NO^-) does not accumulate in detectable amounts during the initial stage of the reaction but is converted to Cbl(III)NO_2 (−3.77 ppm) by oxygen present in the sample. Nitrosylcobalamin appears, however, during the later reaction stage[30] (trace B in Figure 3b), and undergoes subsequent slow conversion to Cbl(III)NO_2 due to the reaction with air oxygen and/or oxidized thiol, RSSR (traces H−I). The other initially formed product with a ^{31}P resonance at −3.95 ppm is assigned to Cbl(III)SG. The intensity of this peak increases slightly during the first several hours of the reaction (traces A−C in Figure 3b) and remains constant during the slow reaction phase.

It is concluded from the UV−vis and NMR data that the reaction of aquacobalamin with GSNO leads to formation of nitrosylcobalamin and glutathionylcobalamin, of which the former product is oxidized to Cbl(III)NO_2 in the presence of O_2. The relative product ratios were observed to vary depending on the exact experimental conditions (mainly excess of nitrosothiol and oxygen content of the sample). For example, the content of Cbl(III)SG in the final reaction mixtures obtained from air-equilibrated samples was noticeably higher as compared to that obtained under strictly oxygen-free conditions. Nevertheless, at pH 7.4, Cbl(III)(NO^-) (or its oxidized form, Cbl(III)NO_2) was the prevailing reaction product under all conditions studied.

The reaction pathways suggested to account for the reactivity pattern observed in the absence of O_2 are summarized in eqs 2−4 of Scheme 2. As shown in the scheme, the initial reaction step involves formation of the intermediates **1a** and **1b**, which decay to the products via heterolytic splitting of the S−NO bond in the S- and N-bonded adducts (reaction paths **a** and **b**, respectively). The reaction path **a**, involving formation of thiolatocobalamin and nitrite, is analogous to that described previously for Hg(II)-catalyzed decomposition of nitrosothiols.[6,31] Formation of an N-bonded intermediate invoked in pathway **b** parallels that suggested for the copper-promoted decomposition of RSNO,[1,2,6] as well as that observed in the reactions of nitroprusside with thiols.[1,6,32] In the present case, heterolytic N−S bond cleavage in **1b** leads to a net transfer of the NO^- group to the Co(III) center and formation of a very stable product Cbl(III)(NO^-) ($K = 1 \times 10^8$ M^{-1}, pH 7.0)[33] (a likely reaction pathway involving decay of the concomitantly formed reactive RS^+ species under the employed experimental conditions is suggested in eq 4). Since Cbl(III) may form stable complexes with both N- and S-donor ligands, it is difficult to assess the preferred mode of GSNO coordination in the initially formed Cbl(III)−RSNO adduct. It is, however, clear from the observed product distribution that the NO^- group transfer represents the main reaction route by which aquacobalamin is converted to the final products. This may possibly reflect

(30) Observation of Cbl(III)(NO^-) in the NMR experiments reported in Figure 3b results from its inefficient conversion to Cbl(III)NO_2 by air oxygen under the specific experimental conditions in the NMR measurement. After depletion of O_2 present in solution, this process is limited by slow diffusion of O_2 from the upper part of the NMR tube (filled with air). Consequently, Cbl(III)(NO^-) formed in the upper layer of the solution in the NMR tube is fully converted into Cbl(III)NO_2 but accumulates in the lower layers close to the bottom of the tube. This contrasts the situation in the UV−vis experiments, where the concentrations of Cbl(III)H_2O used were ca. 2 orders of magnitude lower than those employed in the NMR studies, and consequently, much smaller amounts of Cbl(III)(NO^-) were formed. The amount of O_2 present in air-saturated solutions was in this case sufficient to effect its rapid and complete oxidation to Cbl(III)NO_2, such that accumulation of Cbl(III)(NO^-) was not observed. The partial conversion of Cbl(III)(NO^-) to Cbl(III)NO_2 in the NMR experiments performed in air-saturated solutions could not be prevented due to the long time scale of the NMR measurements necessitated by the slow kinetics of the reaction with GSNO. Nevertheless, this does not in any way invalidate the main conclusions concerning the reaction of Cbl(III)H_2O with GSNO provided in the Discussion.

(31) (a) Swift, H. R.; Williams, D. L. H. *J. Chem. Soc., Perkin Trans. 2* **1997**, 1933. (b) McAninly, J.; Williams, D. L. H.; Askew, S. C.; Butler, A. R.; Russel, C. *J. Chem. Soc., Chem. Commun.* **1993**, 1758.
(32) Szaciłowski, K.; Wanat, A.; Barbieri, A.; Wasielewska, E.; Witko, M.; Stochel, G.; Stasicka, Z. *New J. Chem.* **2002**, *26*, 1495.
(33) Zheng, D.; Birke, R. *J. Am. Chem. Soc.* **2001**, *123*, 4637.

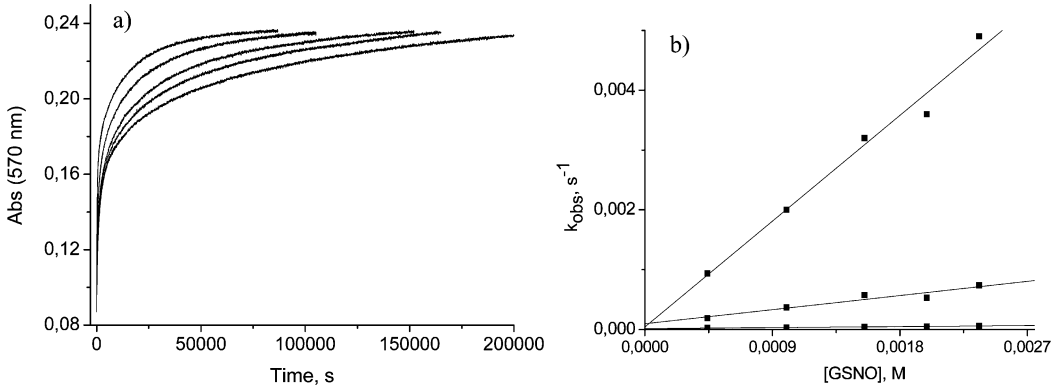

Figure 4. (a) Absorbance/time plots featuring the reaction of Cbl(III)H_2O with GSNO in the presence of O_2. (b) Plots of k_{obs} versus [GSNO] obtained for steps 1−3 from three-exponential fits of kinetic traces measured at various [GSNO]. Experimental conditions: [Cbl(III)H_2O] = 5×10^{-5} M, pH 7.4 (0.1 M Tris), 25 °C.

the preference of the Co(III) center for the formation of the N-bonded intermediate.

On the basis of the UV−vis and NMR data, it is tentatively concluded that the UV−vis spectral evolution featuring the first reaction step in the absence of O_2 (compare inset in Figure 2a) reflects formation of Cbl(III)−RSNO adducts **1a** and/or **1b** and relatively rapid (on a time scale of minutes) conversion of **1a** to Cbl(III)SR, while the slower step reflects formation of Cbl(III)(NO^-) (pathway **b** of Scheme 2). This reactivity pattern is further complicated in the presence of O_2 due to a gradual conversion of Cbl(III)(NO^-) to Cbl(III)NO_2 (reaction 5 of Scheme 2), which occurs at a rate and to an extent that depends on the oxygen content of the sample. Furthermore, since the stability constant of Cbl(III)NO_2 ($K = 2.3 \times 10^5$ M^{-1})[33,35] is much smaller than that of Cbl(III)(NO^-), conversion of Cbl(III)(NO^-) to Cbl(III)NO_2 likely disturbs the initial product ratio and leads to subsequent slow equilibration processes involving readjustment of Cbl(III)NO_2 and Cbl(III)SG concentrations (as evidenced by a slow increase in the Cbl(III)SG concentration observed by NMR in air-equilibrated samples).

The processes associated with oxidation of Cbl(III)(NO^-) complicate reliable kinetic analysis of the system. This was indicated by the UV−vis kinetic studies performed in an excess of GSNO. The initial measurements involved analysis of temporal UV−vis spectral changes recorded under oxygen-free conditions. Analysis of the kinetic traces obtained under such conditions was, however, difficult due to the interference of trace amounts of oxygen, which affected the character and magnitude of the observed spectral changes. As a consequence, the rate constants $k_{obs}(1)$ and $k_{obs}(2)$ obtained by fitting the kinetic traces measured at different initial [GSNO] to two-exponential functions were considerably scattered (compare Figure S2). Further kinetic studies were performed for air-saturated solutions. The kinetic traces observed under such conditions (compare Figure 4a) required numerical analysis by a three-exponential model. Fits of the traces gave three components from which the rate constants $k_{obs}(1)$, $k_{obs}(2)$, and $k_{obs}(3)$, respectively, were determined at different [GSNO]. Plots of the k_{obs} values versus [GSNO] (Figure 4b) allowed determination of the rate constants $k_1 = 2.0 \pm 0.2$ M^{-1} s^{-1}, $k_2 = 0.26 \pm 0.05$ M^{-1} s^{-1}, and $k_3 = (1.9 \pm 0.1) \times 10^{-2}$ M^{-1} s^{-1}. Due to a rather complex pattern of reaction pathways followed by the reactants in the presence of oxygen, an unambiguous assignment of the processes associated with the three kinetically observed steps is difficult. Nevertheless, the similarity of the second-order rate constants determined for the first and second reaction steps in the presence of oxygen to those estimated from measurements in deoxygenated samples (viz. $k_1' = 1.1 \pm 0.1$ M^{-1} s^{-1} and $k_2' = 0.13 \pm 0.02$ M^{-1} s^{-1}, Figure S2) suggests a similarity in the nature of the processes that determines the kinetics of steps 1 and 2 in the presence and absence of O_2. It is tentatively concluded that step 1 reflects the kinetics of formation of intermediates **1a** and **1b** and conversion of **1a** to Cbl(III)SG (Scheme 2), while the two slower steps are mainly associated with formation of Cbl(III)NO_2 (i.e., eq 3 followed by eq 5) and equilibration processes leading to a slow increase in the concentration of Cbl(III)SG.

Reaction of Cbl(III)H_2O with *S*-Nitroso-*N*-acetylpenicillamine. The reactivity pattern observed for the tertiary nitrosothiol SNAP was more straightforward than that observed for GSNO. Figure 5 reports typical spectral changes accompanying the reaction under oxygen-free conditions. As can be seen from these data, mixing of the reactants results in a rapid small spectral shift, followed by substantial changes in the spectrum that indicate formation of Cbl(III)(NO^-) as the ultimate cobalamin product. Due to a relatively rapid rate of the reaction (as compared to that observed for GSNO), attempts to characterize reaction intermediates by NMR spectroscopy were not successful. The first NMR spectrum recorded at the reactant concentrations required for NMR measurements was virtually identical with that of Cbl(III)(NO^-) (vide infra). Formation of an intermediate was, however, evident from the initial rapid change in the UV−vis spectrum of aquacobalamin resulting from mixing of the reactants. The observed increase in the magnitude of this shift on increasing [SNAP] is indicative of the initial rapid ($t_{1/2}$ < 30 s) equilibration reaction (6a), followed by the slower formationof Cbl(III)(NO^-) (reaction 6b; P = products

(34) Firth, R. A.; Hill, H. A. O.; Pratt, J. M.; Thorp, R. G.; Williams, R. J. P. *J. Chem. Soc. A* **1969**, 381.
(35) Zheng, D.; Yan, L.; Birke, R. L. *Inorg. Chem.* **2002**, *41*, 2548.

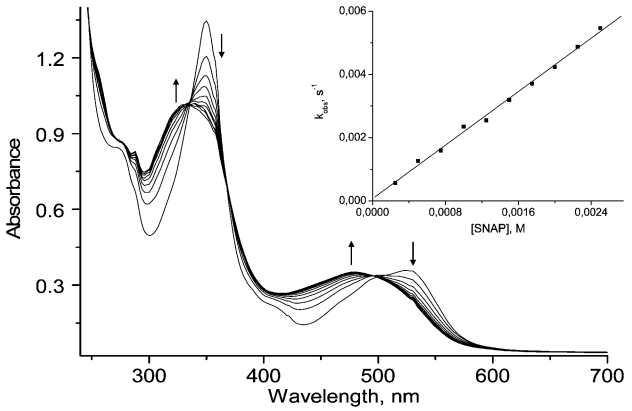

Figure 5. Spectral changes accompanying the reaction of aquacobalamin (5×10^{-5} M) with SNAP (2.5×10^{-4} M) in the absence of O_2. Experimental conditions: pH 7.4 (0.1 M phosphate buffer), overall reaction time 80 min. Inset: plot of k_{obs} versus [SNAP] for the reaction of aquacobalamin (4×10^{-5} M) with SNAP (oxygen-free conditions, pH 7.4, 22 °C).

of nitrosothiol decomposition).

$$Cbl(III)H_2O + RSNO \overset{fast}{\rightleftharpoons} Cbl(III)-RSNO + H_2O \quad (6a)$$

$$Cbl(III)-RSNO \rightarrow Cbl(III)(NO^-) + P \quad (6b)$$

The kinetics of the subsequent step (eq 6b) was studied by UV−vis spectroscopy at [SNAP] ≥ 10 [Cbl(III)H_2O]. The absorbance/time plots featuring the reaction under oxygen-free conditions gave good mathematical fits to a single-exponential function. A plot of the resulting k_{obs} values versus [SNAP] was linear in the studied range of concentrations (inset in Figure 5). A fit of the data allowed determination of the second-order rate constant $k_4 = 2.11 \pm 0.05$ M^{-1} s^{-1}. No meaningful intercept was obtained from the plot, indicating that the reaction is effectively irreversible under the employed experimental conditions.

When the same reaction was carried out in the presence of oxygen, a relatively rapid ($t_{1/2} < 5$ min at [SNAP] = 1×10^{-3} M) quantitative conversion of Cbl(III)H_2O to Cbl(III)-NO_2 was observed. ^{31}P NMR spectra of the Cbl(III)H_2O and SNAP solutions reacted in the absence and presence of O_2 indicated formation of Cbl(III)(NO^-) and Cbl(III)NO_2, respectively, as the final cobalamin product. The corresponding ^{1}H NMR spectra evidenced formation of trace amounts of Cbl(III)SR adduct with an axially coordinated *N*-acetylpenicillamine as the additional residual product (compare Figure S3). The amounts of thiolato adduct were, however, substantially smaller than those formed in the reaction with GSNO at the same pH.

The different reactivity pattern and final product distribution observed in the reaction of aquacobalamin with GSNO and SNAP, respectively, likely reflect the lower stability of the Co(III)−S bond formed by SNAP (and the corresponding thiol *N*-acetylpenicillamine) as compared to that formed by GSNO (and glutathione, GSH). In fact, the apparent stability constant determined for the thiolato adduct of cobalamin with NAP ($K = (3.3 \pm 0.7) \times 10^3$ M, 25 °C, pH 7.4, compare Figure S4) is significantly smaller than that estimated for Cbl(III)SG in air-saturated solution ($K = 1.1 \times 10^5$ M^{-1}, 25 °C, pH 5.5).[28a] This result is in line with expectations based on the point charge calculations reported for both nitrosothiols,[22] which suggest a more nucleophilic nature of the S atom in GSNO (Figure 6). Our experimental observations and the above-mentioned theoretical calculations justify the assumption that formation of the S-bonded Cbl(III)S(NO)R intermediate is more favorable in the case of GSNO, whereas a lower nucleophilic character and a larger steric hindrance around the sulfur atom in SNAP may favor an N-bonded adduct in the reaction of Cbl(III)H_2O with SNAP. Consequently, pathway **b** of Scheme 2 is likely preferred in the interaction of aquacobalamin with SNAP. Notably, a much faster rate of Cbl(III)(NO^-) formation observed in the reaction with SNAP as compared to that with GSNO possibly reflects a lower activation barrier for the heterolytic S−NO bond cleavage in the N-bonded adduct formed by SNAP due to a better stabilization of the transient RS^+ species formed from this tertiary nitrosothiol as compared to the highly unstable primary RS^+ formed by decomposition of GSNO.

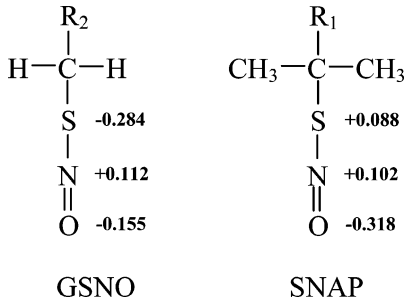

Figure 6. Point charges calculated for the S−N═O group in GSNO and SNAP (data from ref 22).

An analogous reactivity pattern apparently involving a net transfer of the NO^- group from coordinated nitrosothiol to the redox-active Fe(III) center has been reported for the reactions of SNAP with the water-soluble iron(III) porphyrins (TMPyP)Fe^{III} and (TPPS)Fe^{III} (eq 7).[9]

$$(Por)Fe^{III} + RSNO \rightarrow (Por)Fe^{II}(NO) + P$$
$$(P = \text{products of nitrosothiol decomposition}) \quad (7)$$

No mechanistic data that would allow elucidation of the possible reaction pathways was, however, provided for these systems.

Although the experimental results obtained in the present work do not reveal intimate mechanistic details of the reactions of Cbl(III)H_2O with RSNO, they provide clear evidence that interaction of aquacobalamin with both GSNO and SNAP leads to decomposition of the nitrosothiols on a time scale of minutes (SNAP) to hours (GSNO). This occurs through cleavage of the S−NO bond in the Cbl−RSNO adducts followed by a net transfer of the NO^- group to the Co(III) center (or, to a smaller extent, formation of Cbl(III)-SR and NO_2^-, path **a** of Scheme 2). Spontaneous release of free NO is not observed. This was confirmed by NO-electrode measurements performed in deoxygenated solutions of the studied nitrosothiols ([RSNO] = 1×10^{-4} M) in which the maximal NO concentrations after addition of aquacobalamin (1×10^{-4} M) did not exceed 2% of that expected

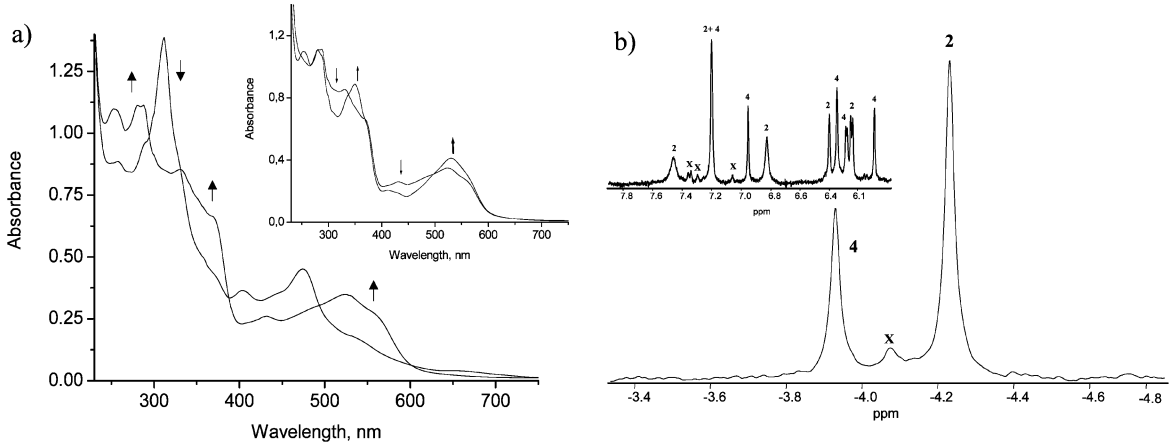

Figure 7. (a) UV−vis spectral change resulting from mixing of deoxygenated solutions of Cbl(II) (5×10^{-5} M) and GSNO (5×10^{-5} M) at pH 7.4 (0.1 M Tris). The inset shows the spectral change resulting from oxidation of the final reaction mixture by air oxygen. (b) ^{31}P NMR spectrum of the products formed in the reaction of Cbl(II) (5×10^{-3} M) with GSNO (7×10^{-3} M) at pD = 7.5 (inset shows an aromatic region of the corresponding ^{1}H spectrum). Resonance assignments: **2**, Cbl(III)(NO$^-$); **4**, Cbl(III)SG (compare Table S1); **X**, not assigned.

for stoichiometric release of NO from GSNO and were even lower (ca 0.3%) in the case of SNAP.

Reactivity of Cbl(II) toward *S*-Nitrosothiols. General Remarks. As indicated by preliminary UV−vis measurements, interaction of Cbl(II) with both studied nitrosothiols involves redox processes leading to reduction of nitrosothiol and concomitant oxidation of cobalamin. Comparison of the standard redox potential for the Cbl(III)/Cbl(II) redox couple (−0.04 V vs Ag/AgCl electrode)[36] with that reported for one-electron reduction of nitrosothiols (−0.98 and −0.97 V vs Ag/AgCl electrode for GSNO and SNAP, respectively)[37] implies initial formation of Cbl(II)−RSNO adducts, a process expected to drastically lower the redox potential associated with oxidation of the Co(II) center (see below). NO-sensitive electrode measurements indicated that the observed redox processes are accompanied by the release of only small amounts of free NO (the maximal NO concentrations amounted to ca. 3% of that expected for quantitative liberation of NO from RSNO). Despite these small amounts, it could be noted that the release of NO from GSNO occurs immediately after addition of Cbl(II), while in the case of SNAP, it takes seconds to minutes. This observation paralleled substantial differences in the kinetics of the Cbl(II) reaction with GSNO and SNAP, respectively. Very fast UV−vis spectral changes accompanying the reaction of Cbl(II) with GSNO contrasted much slower ones observed for SNAP. The studies described below were performed to elucidate the pathways involved in the observed reactions and to estimate factors which likely contribute to the differences in the reactivity of GSNO and SNAP toward Cbl(II).

Reaction of Cbl(II) with GSNO. Mixing of Cbl(II) and GSNO in the absence of O_2 results in formation of Cbl(III)SG and Cbl(III)(NO$^-$) (Figure 7). The reaction occurs close to the upper limit of rates accessible with the stopped-flow technique. Stopped-flow kinetic measurements were performed at 5 °C and in a low concentration range of GSNO, $(2-6) \times 10^{-4}$ M. The absorbance/time plots obtained under such conditions gave good mathematical fits to one-exponential functions, allowing determination of k_{obs} at various [GSNO]. The resulting linear plot of k_{obs} versus [GSNO] (Figure 8a) indicate that the reaction is first-order with respect to [GSNO]. However, since a significant portion of the reaction (ca 30%) occurred within the mixing time of the instrument (5 ms), the determined k_{obs} values are admittedly imprecise and allow only a crude estimation of the second-order rate constant, $k_5 = (1.2 \pm 0.1) \times 10^6$ M^{-1} s^{-1} for the observed reaction.

Equations 8−9 outline the likely pathways followed by reactants in the observed redox process.

$$\text{Cbl(II)} + \text{RSNO} \underset{}{\overset{K_A}{\rightleftharpoons}} \text{Cbl(II)-S}\begin{matrix}\diagup \text{NO} \\ \diagdown \text{R}\end{matrix} \overset{k_B}{\underset{k_{-B}}{\rightleftharpoons}} \text{Cbl(III)SR} + \text{NO} \quad (8)$$

$$\text{NO} + \text{Cbl(II)} \longrightarrow \text{Cbl(III)(NO}^-\text{)} \qquad k_{NO} = 7 \times 10^8 \text{ M}^{-1} \text{ s}^{-1} \quad (9)$$

The first reaction step in eq 8 may, in general, proceed via the S- or N-bonded intermediate. However, due to a very soft nature of the Co(II) center in Cbl(II),[38] the initial S- rather than N-binding of nitrosothiol is assumed to be the preferred coordination mode. As indicated by cyclic voltammetry measurements, coordination of glutathione to Cbl(III)H_2O shifts the one-electron reduction potential of the Co(III) center from −0.04 to ca −0.98 V (vs Ag/AgCl reference electrode, compare Figure S5, Supporting Information). Formation of the Cbl(II)−S(NO)R intermediate should result in a similar large negative shift of the Co(III)/Co(II) redox potential, thus providing the driving force for oxidation of the Co(II) center to the highly stabilized Cbl(III)SR species (and concomitant release of free NO), as shown in eq 8. Notably, the reversible reaction 8 is analogous to that reported for the interaction of nitrosothiols with selected

(36) Lexa, D.; Saveant, J. M. *Acc. Chem. Res.* **1983**, *16*, 235.
(37) Hou, Y.; Wang, J.; Arias, F.; Echegoyen, L.; Wang, P. G. *Bioorg. Med. Chem. Lett.* **1998**, *8*, 3065.
(38) Balasubramanian, P. N.; Gould, E. S. *Inorg. Chem.* **1985**, *24*, 1791 and references therein.

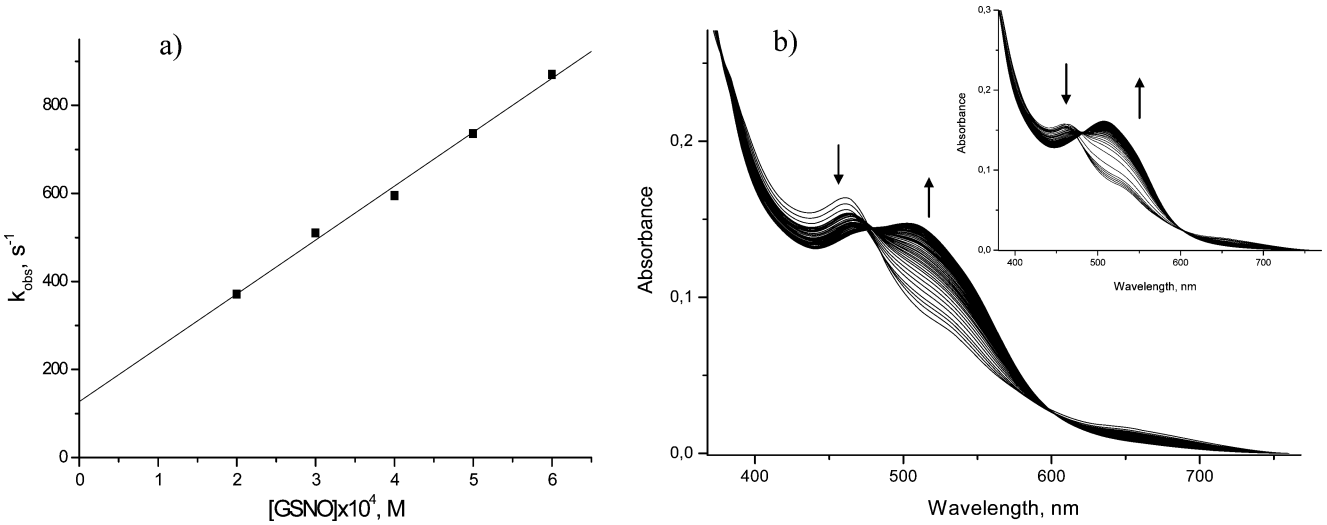

Figure 8. (a) Plot of k_{obs} versus [GSNO] for the reaction of Cbl(II) (2×10^{-5} M) with GSNO at pH 7.4 and 5 °C. (b) Rapid-scan UV−vis spectra recorded for the reaction of Cbl(II) (ca 2×10^{-5} M) with GSNO (5×10^{-4} M) in buffered MeOH/H_2O mixture (pH 7.4, 0.05 M Tris) at −40 °C. The spectra were recorded within the time 45 ms to 9 s after mixing of the reactants. The inset shows the corresponding spectral changes observed at a higher GSNO concentration (1×10^{-3} M) (overall reaction time 9 s).

copper complexes in which the Cu center catalyses nitrosothiol decomposition, or its formation from RSH (eq 10)

$$\text{(L)Cu(I)} + \text{RSNO} \rightleftharpoons \text{(L)Cu(I)-S}\begin{matrix}\text{NO}\\ \diagup\\ \diagdown\\ \text{R}\end{matrix} \rightleftharpoons \text{(L)Cu(II)SR} + \text{NO} \qquad (10)$$

depending on the actual reaction conditions.[39]

The low concentrations of free NO in solution detected by the NO electrode and rapid formation of significant amounts of Cbl(III)(NO^-) as one of the reaction products indicate that the released NO is rapidly and efficiently scavenged by unreacted Cbl(II) ($k_{NO} \approx 7 \times 10^8$ M^{-1} s^{-1}, $K_{NO} = 1 \times 10^8$ M^{-1}, eq 9),[26b,33] thus shifting the equilibrium in eq 8 to the right.

On the basis of the literature data on the reactivity of Cbl(II), the first equilibrium in reaction 8 should be very fast[26b,40] and exhibit a small value of K_A.[35,41−42] Assuming electron transfer to be rate-limiting, the observed rate constant for reaction 8 is described by eq 11a.

$$k_{obs} = \frac{k_B K_A[\text{GSNO}]}{1 + K_A[\text{GSNO}]} + k_{-B}[\text{NO}] \qquad (11a)$$

Due to the subsequent rapid step (eq 9) which makes the overall reaction effectively irreversible, the contribution of the reverse reaction (term k_{-B}[NO] in eq 11a) to k_{obs} can be neglected. Thus, eq 11a simplifies to eq 11b, which predicts leveling off of k_{obs} at high [GSNO] (eq 11d).

$$k_{obs} = \frac{k_B K_A[\text{GSNO}]}{1 + K_A[\text{GSNO}]} \qquad (11b)$$

$$K_A[\text{GSNO}] \ll 1: \quad k_{obs} = k_B K_A[\text{GSNO}] \qquad (11c)$$

$$K_A[\text{GSNO}] \gg 1: \quad k_{obs} = k_B \qquad (11d)$$

The experimentally determined linear dependence of k_{obs} versus [GSNO] indicates that in the studied range of GSNO concentrations eq 11c is valid,[43] such that the second-order rate constant estimated from the slope of the plot in Figure 8a, $k_5 = 1.2 \times 10^6$ M^{-1} $s^{-1} \approx k_B K_A$. Due to a very limited range of [GSNO] at which the reaction kinetics could be measured, the proposed reaction scheme could not be verified kinetically by measuring k_{obs} at high [GSNO]. The rapid reaction rate also precludes distinction of the two reaction steps assumed in eq 8. Evidence in support of the proposed scheme was, however, obtained from low-temperature stopped-flow measurements performed at −40 °C in 70% v/v methanol/water mixture buffered to pH 7.4 (0.05 M Tris). Rapid-scan measurements performed at [GSNO] = (3−13) $\times 10^{-4}$ M indicated the occurrence of an initial spectral shift in the electronic spectrum of Cbl(II) (compare Figure 8b), which, on the basis of the magnitude and type of spectral change,[44] is assumed to reflect the first equilibrium of eq 8. This was followed by oxidation of the Co(II) center to a mixture of Cbl(III)SG and Cbl(III)(NO^-). A more complex pattern of spectral changes observed at [GSNO] ≥ 1×10^{-3} M (indicating the occurrence of three subsequent

(39) (a) Stubauer, G.; Giuffré, A.; Sarti, P. *J. Biol. Chem.* **1999**, *274*, 28128. (b) Inoue, K.; Akaike, T.; Miyamoto, Y.; Okamoto, T.; Sawa, T.; Otagiri, M.; Suzuki, S.; Yoshimura, T.; Maeda, H. *J. Biol. Chem.* **1999**, *274*, 27069. (c) Pawelec, M.; Stochel, G.; van Eldik, R. *Dalton Trans.* **2004**, 292.

(40) (a) Bakac, A.; Espenson, J. H. *Inorg. Chem.* **1989**, *28*, 4319 (b) Mulac, W. A.; Meyerstein, B. *J. Am. Chem.* Soc. **1982**, *104*, 4123.

(41) This assumption is based on the observed low affinity of Cbl(II) for the sixth ligand, as evidenced by the small values of the binding constant $K_{eq} = [\text{Cbl(II)L}]/[\text{Cbl(II)}][\text{L}] \leq 300$ M^{-1} reported for ligands such as CN^-, NO_2^-, RS^-, and RSH.[35,41b−c,42] Additional evidence comes from cyclic voltammetric studies which indicated low affinity of glutathione and *N*-acetylpenicillamine toward the Co(II) center in reduced cobalamin. Due to the presence of the nitrosyl group coordinated to the sulfur atom, even lower affinity is expected for the corresponding adducts with RSNO (in analogy to the difference in the stability of Cbi(II)S(H)R and Cbi(II)SR adducts formed by cobinamide and 2-mercaptoethanol, for which stability constants 2.5×10^3 and 11.5 M^{-1}, respectively, were reported[42]). (b) Lexa, D.; Saveant, J. M.; Zickler, J. *J. Am. Chem. Soc.* **1980**, *102*, 2654. (c) Law, P. Y.; Wood, J. M. J. *Am. Chem. Soc.* **1973**, *95*, 914.

(42) Cockle, S.; Hill, H. A. O.; Ridsdale, S.; Williams, R. J. P. *J. Chem. Soc., Dalton Trans.* **1972**, 303 and references therein.

Scheme 3

$$\text{Cbl(III)SR + NO} \underset{k_B}{\overset{k_{-B}}{\rightleftharpoons}} \text{Cbl(III)S(NO)R} \overset{K_A}{\rightleftharpoons} \text{Cbl(II) + RSNO} \quad (12)$$

$$\text{Cbl(II)} \xrightarrow{\text{fast}} \text{Cbl(III)(NO}^-\text{)} \quad (+\text{NO})$$

$$\text{Net reaction: Cbl(III)SR + 2NO} \longrightarrow \text{Cbl(III)(NO}^-\text{) + RSNO} \quad (13)$$

processes, inset in Figure 8b) possibly reflects an additional reaction route involving outer-sphere electron transfer (as observed for SNAP, vide infra). Although the overall reaction pattern in the MeOH/H_2O cryosolvent is not expected to differ substantially from that occurring in water, the detailed kinetic data obtained in this medium are of little biological relevance. Thus, no in-depth kinetic studies were performed under these conditions.

According to eq 8, Cbl(II)-induced decomposition of GSNO should be reversible in the absence of efficient NO scavengers. In fact, the kinetics of the reverse reaction 12 can be studied separately by reacting Cbl(III)SG with excess NO as shown in Scheme 3.

Due to the potential biological importance of this reaction,[21] its kinetics was recently studied by Birke at al.[21] The mechanistic scheme assumed in these studies (i.e., direct attack of NO at the Co(III) center leading to the formation of Cbl(III)(NO^-) and $GS^\bullet$, eq 1) is slightly different from that depicted in eq 12. In our opinion, reaction of Cbl(III)-SG with NO is likely described by the reversible equilibrium (eq 12), which in the presence of a large excess of NO becomes effectively irreversible. To reveal the mechanistic features of the reaction, we have studied its kinetics as a function of temperature and pressure to determine the activation parameters $\Delta H^\ddagger$, $\Delta S^\ddagger$, and $\Delta V^\ddagger$. Mixing of deoxygenated solutions of Cbl(III)SG and NO ([NO] $\geq$ 10[Cbl-(III)SG]) leads to a rapid and quantitative conversion of glutathionylcobalamin to Cbl(III)(NO^-) (Figure 9), in agreement with the reaction sequence in Scheme 3. Since in the present system equilibrium K_A is expected to be fast, k_{-B} is rate-limiting and the k_{obs} values measured under excess NO are expressed by eq 14.

$$k_{obs} = k_{-B}[NO] \quad (14)$$

Plots of k_{obs} (obtained by fitting the kinetic traces at 560 nm to one-exponential functions) versus [NO] were linear with intercepts at the origin, in agreement with eq 14. The value of the second-order rate constant $k_{-B} = (2.58 \pm 0.08) \times 10^3$ M^{-1} s^{-1} (25 °C; inset in Figure 9) agrees well with that previously reported (viz. 2.82×10^3 M^{-1} s^{-1}).[21] The

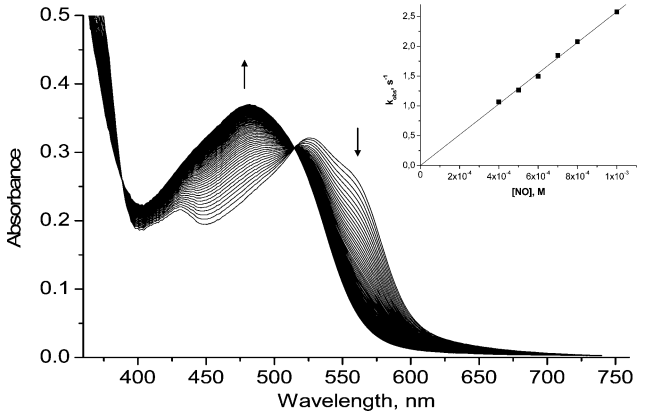

Figure 9. Rapid-scan UV−vis spectra recorded for the reaction of glutathionylcobalamin (5×10^{-5} M) with NO (1×10^{-3} M) at pH 7.0 (0.1 M phosphate buffer). Overall reaction time 2 s. Inset: plot of the observed rate constants (at 25 °C) versus [NO].

k_{-B} values determined in the temperature range 11−35 °C were used to construct the Eyring plot (Figure S6a), from which the activation parameters $\Delta H^\ddagger = 41 \pm 3$ kJ mol^{-1} and $\Delta S^\ddagger = -42 \pm 9$ J mol^{-1} K^{-1} were obtained. The significantly negative $\Delta S^\ddagger$ value suggests that the reaction of glutathionylcobalamin with NO follows an associative pathway. This was confirmed by studies on the effect of hydrostatic pressure (10−130 MPa) on the reaction rate, which yielded the activation volume $\Delta V^\ddagger = -9.6 \pm 0.3$ cm^3 mol^{-1} (Figure S6b). The results are consistent with the mechanism depicted in eq 15.

$$\text{Cbl(III)SR + NO} \overset{\text{rds}}{\rightleftharpoons} \left[\text{Cbl(III)}\!-\!\text{S}\!<^{\text{R}}_{\text{NO}^\bullet}\right]^\ddagger \overset{\text{fast}}{\rightleftharpoons} \text{Cbl(II) + RSNO} \quad (15)$$

In accordance with the principle of microscopic reversibility, the process depicted in (eq 15) involves the same elementary steps as those assumed for the interaction of Cbl-(II) with RSNO in eq 8, i.e., rapid formation of an S-bonded Cbl(II)−RSNO adduct, and the rate-determining electron-transfer accompanied by the release of NO. Notably, a mechanism similar to that described by eq 8 has been proposed for the reactions of nitrosothiols with model ruthenium and osmium porphyrins.[5,7,13] In addition, the reaction sequence assumed in (eq 15) parallels that suggested recently for the reversible S-nitrosation of the thiolato-ligated Fe(III) heme center in a NO transport protein, cNP (*Cimex lectarius* nitrophorin, Scheme 4a).[45]

The negative $\Delta S^\ddagger$ and $\Delta V^\ddagger$ values determined in the present study for NO binding to Cbl(III)SG are similar to those reported recently for nitrosylation of the thiolato ligand in the model ferriheme complex (P)Fe^{III}(NO)(SR) (viz. $\Delta S^\ddagger = -96$ J mol^{-1} K^{-1} and $\Delta V^\ddagger = -16.3$ cm^3 mol^{-1}, respectively,

(43) The intercept of the linear plot reported in Figure 8a suggests a contribution from the reversible reaction k_{-B}[NO] to the observed rate constant. This, however, likely results from an experimental error associated with the stopped-flow measurements of the very rapid reaction 8. It could be observed in the performed experiments that on increasing [GSNO], an increasing portion of the reaction occurred within the mixing time of the instrument. This presumably leads to a gradual decrease in the observed rate constants obtained by fitting the measurable part of the trace to a single-exponential function. Such an effect is expected to result in an artifact intercept in the plot of k_{obs} vs [GSNO]. Reliable evaluation of the experimentally observable intercept is further complicated by a narrow range of GSNO concentrations in which the reaction could be studied.

(44) Similar small rapid spectral shift featuring coordination of a ligand to the Co(II) center in reduced cobalamin has been observed as the initial step in the reaction of Cbl(II) with L = $[Fe(CN)_5NO]^{3-}$ and $[Fe(CN)_6]$,$^{4-}$ compare Wolak, M.; Stochel, G.; van Eldik, R. *J. Am. Chem. Soc.* **2003**, *125*, 1334.

(45) (a) Weichsel, A.; Maes, E. M.; Andersen, J. F.; Valenzuela, J. G.; Shokhireva, T. Kh.; Walker, F. A.; Montfort, W. R. *Proc. Natl. Acad. Sci. U.S.A.* **2005**, *102*, 594. (b) Walker, F. A. *J. Inorg. Biochem.* **2005**, *99*, 216.

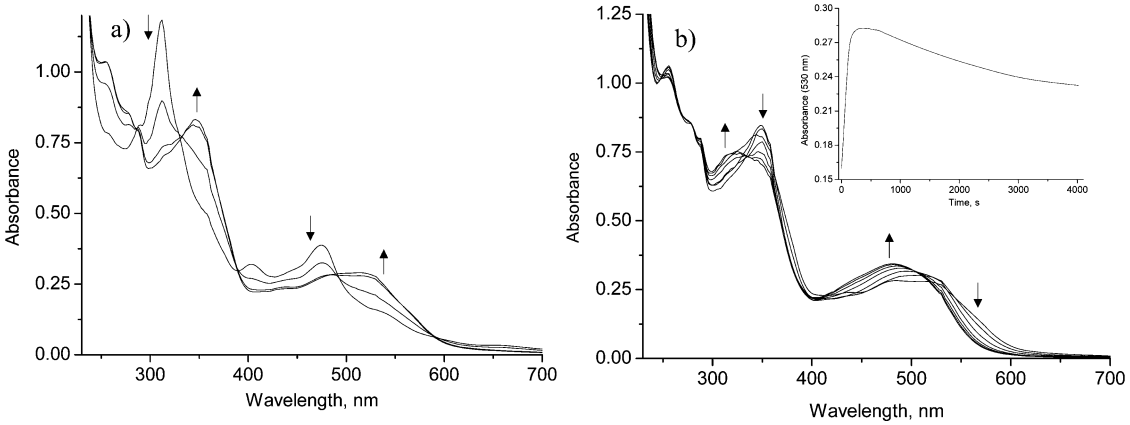

Figure 10. UV−vis spectral changes accompanying the reaction of Cbl(II) (5×10^{-5} M) with SNAP (5×10^{-5} M) at pH 7.4: (a) 0−3 min (b) 3−80 min after mixing of the reactants. Inset shows the time evolution of the absorbance at 530 nm (temp. 25 °C).

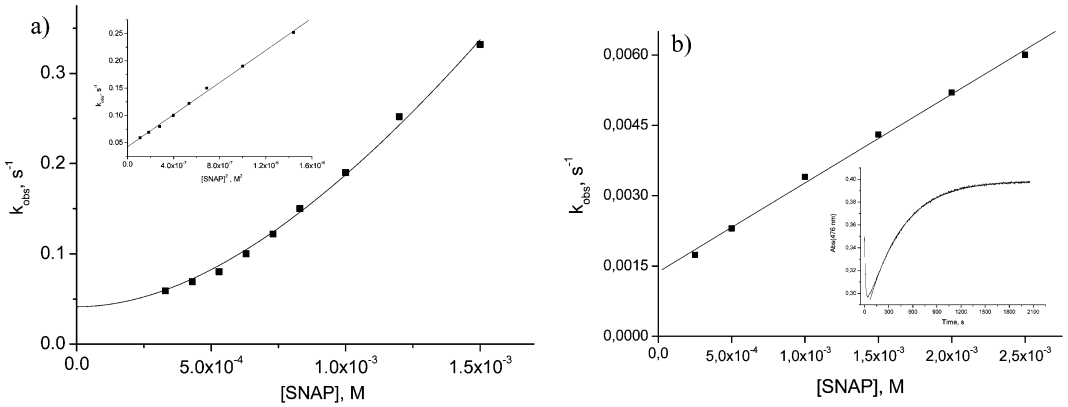

Figure 11. (a) Plot of $k_{obs}(1)$ versus [SNAP] and [SNAP]^2 (inset) measured for the first step of the reaction of Cbl(II) with SNAP at 25 °C (pH 7.4, 0.1 M Tris) in the absence of O_2. (b) Plot of $k_{obs}(2)$ versus [SNAP] determined for the second step of the reaction under oxygen-free conditions ([Cbl(II)] = 2.5×10^{-5} M, pH 7.4, 22 °C). Inset: fit of the kinetic trace measured at 476 nm and [SNAP] = 5×10^{-4} M to a one-exponential function.

Scheme 4

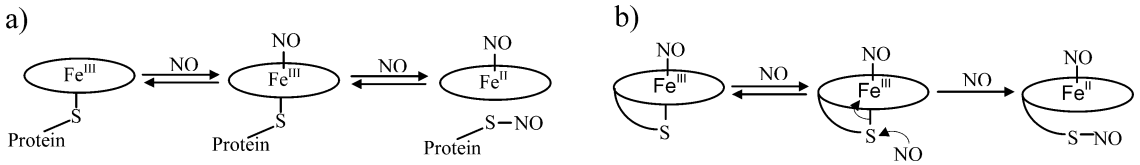

Scheme 4b),[46] strongly suggesting a common associatively activated pathway for both reactions.

Reaction of Cbl(II) with SNAP. The reaction of Cbl(II) with SNAP is much slower as compared to that with GSNO and proceeds in two steps. The first step involves relatively rapid (time scale of seconds) oxidation of Cbl(II) to a mixture of Cbl(III)(NO^-) and sulfur-bound cobalamin derivative(s) (compare Figure 10a). The subsequent slower step involving quantitative conversion of the initially formed cobalamin products to Cbl(III)(NO^-) precludes their identification by NMR spectroscopy. Their nature, however, can be inferred from the UV−vis data. Initial formation of Cbl(III)(NO^-) as one of the products was confirmed by rapid oxidation of the reaction mixture obtained after the first step by air oxygen, which resulted in conversion of Cbl(III)(NO^-) to Cbl(III)NO_2. The presence of substantial amounts of sulfur-bound Cbl(III) species as the other initial product is evident from the nature of the intermediate UV−vis spectrum (Figure 10a), which resembles that observed for the thiolato adduct Cbl(III)SR (SR = *N*-acetylpenicillamine, λ_{max} = 258, 345, 530, and 570 nm, compare Figure S4). The S-bound cobalamin(s) is(are) subsequently converted to Cbl(III)(NO^-) (slow step, Figure 10b) identified by NMR spectroscopy as the ultimate reaction product.

The reaction steps 1 and 2 could be easily separated in terms of observing their kinetics. The absorbance/time plots obtained for the first step in stopped-flow kinetic studies performed in excess SNAP gave satisfactory mathematical fits to one-exponential functions. The observed rate constants exhibited a square dependence on [SNAP] (Figure 11a). The value of the termolecular rate constant $(1.47 \pm 0.27) \times 10^4$ M^{-2} s^{-1} and a positive intercept, (0.043 ± 0.002) s^{-1}, were determined from the linear plot of $k_{obs}(1)$ versus [SNAP]^2 (Figure 11a, inset). The spectral changes characterizing step 2 were followed by conventional UV−vis spectroscopy. The kinetic traces recorded for this step were one-exponential.

(46) Franke, A.; Stochel, G.; Suzuki, N.; Higuchi, T.; Okuzono, K.; van Eldik, R. *J. Am. Chem. Soc.* **2005**, *127*, 5360.

Scheme 5

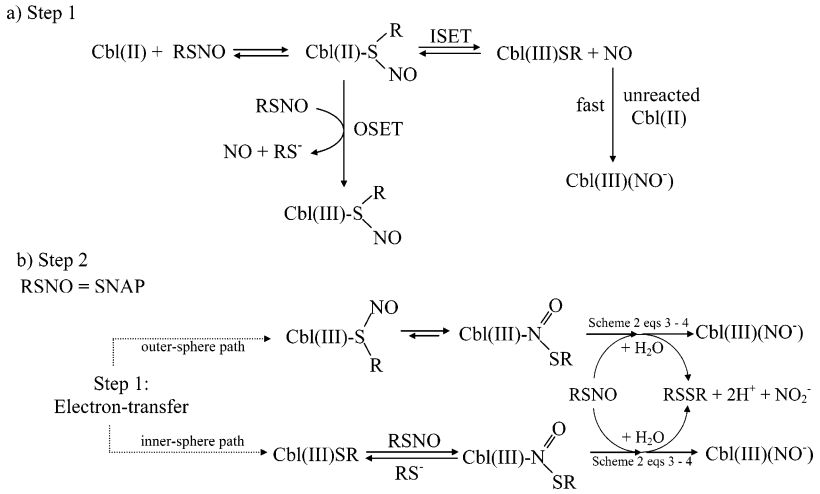

A plot of the observed rate constants $k_{obs}(2)$ versus [SNAP] proved to be linear in the studied range of nitrosothiol concentrations (Figure 11b) and allowed determination of the second-order rate constant $(1.8 \pm 0.1)\ M^{-1}\ s^{-1}$.

Scheme 5 summarizes the reaction pathways suggested to account for the observed reactivity. As indicated in Scheme 5a, the first reaction step is suggested to involve rapid formation of a Cbl(II)−S(NO)R intermediate followed by rate-determining electron transfer. The latter process may in principle follow an inner- or outer-sphere path (denoted in Scheme 5 as 'ISET' and 'OSET', respectively). For the inner-sphere path a linear dependence of k_{obs} on [RSNO] is expected, while the outer-sphere path (involving attack of the second RSNO molecule on the initially formed Cbl(II)S-(NO)R adduct) would result in $k_{obs} \sim [RSNO]^2$. The linear dependence of k_{obs} on $[SNAP]^2$ observed experimentally (Figure 11a, inset) implies that the inner-sphere path is either much less efficient than the dominant outer-sphere reaction or does not occur under the employed experimental conditions ([SNAP]/[Cbl(II)] ≥ 10). However, since the occurrence of inner-sphere electron transfer at low nitrosothiol concentrations ([SNAP] ≈ [Cbl(II)]) cannot be excluded on the basis of the available experimental results, this reaction route was also included in Scheme 5a. Taking into account the assumed primary products formed in the outer- and inner-sphere electron-transfer steps (viz. Cbl(III)S(NO)R, Cbl(III)-SR, and Cbl(III)(NO^-)), the reactions outlined in Scheme 5b are suggested to account for the subsequent slow formation of Cbl(III)(NO^-).

Comparison between GSNO and SNAP in Terms of the Overall Reaction Mechanism. Studies on the reaction of Cbl(II) with GSNO and SNAP indicate a common reaction pattern that involves initial Cbl(II)−RSNO adduct formation followed by an electron-transfer step. The rate and mechanism of the overall reaction, however, strongly depend on the structural and electronic properties of the nitrosothiols. This may reflect both the efficiency of Cbl(II)−RSNO adduct formation (which is expected to be smaller for the bulky tertiary nitrosothiol SNAP as compared to GSNO), as well as the kinetics and thermodynamics of the subsequent electron transfer step. With regard to the latter, inner-sphere electron transfer is apparently efficient in the Cbl(II)−RSNO adduct formed by GSNO but is strongly suppressed (or is not operative) in the reaction of Cbl(II) with SNAP, which under the conditions used in the kinetic study proceeds through an outer-sphere path. Taking into account the sensitivity of inner-sphere electron transfer on the nature (i.e., energies and symmetry) of the molecular orbitals within the bridging groups through which the electrons are transferred, the observed variation in the reaction mechanism may reflect the different electronic properties of the S−N═O linkage in the GSNO and SNAP adducts of Cbl(II) (as suggested by different charge distribution within these groups,[22] Figure 6). In addition, although S coordination of nitrosothiols to the 'soft' Co(II) center is highly probable, N coordination of SNAP (which may be favored for this nitrosothiol) can possibly occur. Such a change in coordination mode would drastically alter the electronic pathways employed by the bridging system in transferring the electrons and therefore affect the rate and mechanism of electron transfer.

Conclusions

The results of the studies on cobalamin−RSNO interactions reported here indicate initial formation of a metal−RSNO adduct. This process serves to activate RSNO toward decomposition, which in the case of Cbl(II) is preceded by electron transfer from the Co(II) center to the nitrosyl group of a nitrosothiol. The observed reaction rates and final cobalamin products depend both on the oxidation state of cobalt and on the nitrosothiol structure. In the latter context, the results obtained for GSNO and SNAP serve as a good illustration of the fact that the reactivity of different RSNOs toward the same metal center may vary significantly from one case to the other.

With regard to the biological relevance of the studied reactions, the conclusions reached can be summarized as follows. Coordination of nitrosothiols to Cbl(III)H_2O promotes slow nitrosothiol decomposition via heterolytic cleavage of the S−N bond. Since, however, the main reaction routes involve in this case the transfer of the −N═O group from RSNO to the Cbl(III) center (where it remains tightly bound in the form of stable Cbl(III)(NO^-) or Cbl(III)NO_2

complexes), interactions with Cbl(III) are not likely to stimulate the NO-donating properties of nitrosothiols. Such a stimulation can, however, occur in the reaction with Cbl(II), which results in nitrosothiol reduction and concomitant release of NO. Nevertheless, it is expected that under in vivo conditions the reverse reaction, i.e., NO binding by glutathionylcobalamin, may be of greater biological relevance. As previously suggested,[21] the latter reaction may have potential therapeutic application in pathophysiological states involving overproduction of NO. As evidenced by mechanistic data obtained in the present study, the intimate mechanism of NO binding to Cbl(III)SG is analogous to that observed for thiolato-ligated iron(III) porphyrin centers, i.e., involves attack of NO at the thiolato ligand followed by reduction of the metal center and concomitant formation of RSNO.

Acknowledgment. The authors gratefully acknowledge financial support from the Deutsche Forschungsgemeinschaft within SFB 583 ("Redox-active metal complexes") and the DAAD/KBN (State Committee for Scientific Research, Poland) Exchange Program.

Supporting Information Available: Reference ^{31}P and ^{1}H NMR data on Cbl(III)H_2O, Cbl(III)(NO^-), Cbl(III)NO_2, and thiolato adducts of Cbl(III) with glutathione and *N*-acetylpenicillamine (Table S1); selected NMR spectra of the products formed in the reaction of Cbl(III)H_2O with GSNO and SNAP, plots of k_{obs} vs [GSNO] for the reaction of Cbl(III)H_2O with GSNO in deoxygenated solution, spectrophotometric determinantion of the stability constant, *K*, for the thiolato adduct of Cbl(III)H_2O with *N*-acetylpenicillamine, cyclic voltammograms of Cbl(III)H_2O and Cbl(III)SG, plots of ln(k/T) vs $1/T$ and ln(k) vs pressure for the reaction of Cbl(III)SG with NO (Figures S1−S6). This material is available free of charge via the Internet at http://pubs.acs.org.

IC051300Q